Acta Pharmaceutica Sinica B 2017;7(3):303–310

Chinese Pharmaceutical Association
Institute of Materia Medica, Chinese Academy of Medical Sciences

Acta Pharmaceutica Sinica B

www.elsevier.com/locate/apsb
www.sciencedirect.com

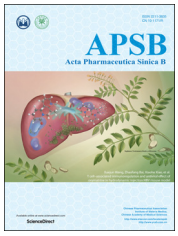

ORIGINAL ARTICLE

Inhibition of protein kinases by anticancer DNA intercalator, 4-butylaminopyrimido[4′,5′:4,5] thieno(2,3-*b*)quinoline

Heggodu G. Rohit Kumar[a], Chethan S. Kumar[b], Hulihalli N. Kiran Kumar[a], Gopal M. Advi Rao[a,*]

[a]*Department of Biochemistry, Davangere University, Shivagangotri, Tholahunase, Davangere 577002, India*
[b]*SS Institute of Medical Sciences and Research Centre, Jnanashankara, Davangere 577005, India*

Received 30 October 2016; received in revised form 2 December 2016; accepted 29 December 2016

KEY WORDS

DNA intercalator;
Molecular docking;
Kinase inhibitor;
Anticancer drugs;
Apoptosis;
Chemotherapy

Abstract Targeting protein kinases (PKs) has been a promising strategy in treating cancer, as PKs are key regulators of cell survival and proliferation. Here in this study, we studied the ability of pyrimido [4′,5′:4,5]thieno(2,3-*b*)quinolines (PTQ) to inhibit different PKs by performing computational docking and *in vitro* screening. Docking studies revealed that 4-butylaminopyrimido[4′,5′:4,5]thieno(2,3-*b*) quinoline (BPTQ) has a higher order of interaction with the kinase receptors than other PTQ derivatives. *In vitro* screening confirms that BPTQ inhibits VEGFR1 and CHK2, with the IC_{50} values of 0.54 and 1.70 μmol/L, respectively. Further, cytotoxicity of BPTQ was measured by trypan blue assay. Treatment with BPTQ decreased the proliferation of HL-60 cells with an IC_{50} value of 12 μmol/L and induces apoptosis, as explicated by the fall in the mitochondrial membrane potential, annexin V labeling and increased expression of caspase-3. Taken together, these data suggest that BPTQ possess ability to inhibit PKs and to induce cell death in human promyelocytic leukemia cells.

*Corresponding author. Tel.: +91 94484 94416.
E-mail address: muttagigopal@yahoo.co.in (Gopal M. Advi Rao).

Peer review under responsibility of Institute of Materia Medica, Chinese Academy of Medical Sciences and Chinese Pharmaceutical Association.

http://dx.doi.org/10.1016/j.apsb.2017.01.001

1. Introduction

Cancer is the major cause of death worldwide. Mutations in the key regulatory genes like proto-oncogenes, tumor suppressor genes, and DNA repair genes are often lead to cancer[1–3]. The basic hallmarks of the cancer, such as the uncontrolled growth, survival, neo-vascularization, metastasis, and invasion, are mainly due to the perturbation of the regulatory signaling pathways[4]. The increasing understanding of molecular pathways altered in cancer diseases has resulted in the development of more specific anticancer agents, referred to as targeted therapies[5,6]. These targeted therapies include the use of monoclonal antibodies and small molecule inhibitors of protein kinases (PKs), which have emerged as promising targets for cancer therapy among several other novel targets identified[7,8].

PKs are key regulators of signal transduction pathways, mediating vital functions, such as cell proliferation, differentiation, and programmed cell death[9]. Also, a number of PKs are associated with different forms of cancers, and plays a prominent role in carcinogenesis. This occurs due to the aberrant activation of PKs, which induce anti-apoptotic effects and promote angiogenesis and metastasis[7,8]. Therefore, inhibitors of these oncogenic PKs are considered as potential anticancer molecules. One of the essential tools in the screening and development of these inhibitors is through structure-based drug design, using *in-silico* analysis and computational chemistry. Over the last several years, studies have yielded many small-molecule tyrosine kinase inhibitors, including numerous quinazoline (saracatinib) and pyrimidine (imatinib) derivatives[10,11]. These drugs act by interacting with their target kinases and blocking its catalytic activity, and are now being used as active candidates in the treatment of a wide range of malignancies like breast, colorectal, lung and pancreatic cancers, lymphoma, leukemia, and multiple myeloma[7,8,11]. Though these molecules possess effective antimalignant activity, we are still in dark to overcome all the tumor forms because of the acquirement of drug resistance. Hence, it is of higher importance to search for novel anticancer compounds targeting kinases to combat cancer.

Earlier in our laboratory, we have studied the ability of pyrimido [4′,5′:4,5]thieno(2,3-*b*)quinoline (PTQ) with amino (APTQ), morpholino (Morpho-PTQ), methoxy (Methoxy-PTQ), oxo (OPTQ) and butylamino (BPTQ) substitutions (Fig. 1) to interact with DNA, and to inhibit cancer cell proliferation[12–16]. Our studies clearly showed that these PTQ derivatives are effective DNA intercalators. Some of the DNA-intercalating anticancer compounds, such as mitoxantrone and anthraquinone derivatives, have displayed kinase inhibitory activity, paving the way for new targets of DNA intercalators[17,18]. It is reported that kinase inhibitory ability will contribute to increase the therapeutic efficacy of DNA binders[17]. Therefore, in this report, we sought to analyze these PTQ derivatives for their ability to inhibit different PKs by performing molecular docking and *in vitro* kinase screening. Results suggest that, 4-butylaminopyrimido[4′,5′:4,5] thieno(2,3-*b*)quinoline (BPTQ) possessed higher interactive ability with the kinases among all the molecules. *In vitro* screening of BPTQ on ten different PKs confirmed that the BPTQ possess inhibitory activity against VEGFR1 and CHK2. Further, cytotoxicity studies revealed that BPTQ induces mitochondrial mediated apoptosis in human promyelocytic leukemia HL-60 cells.

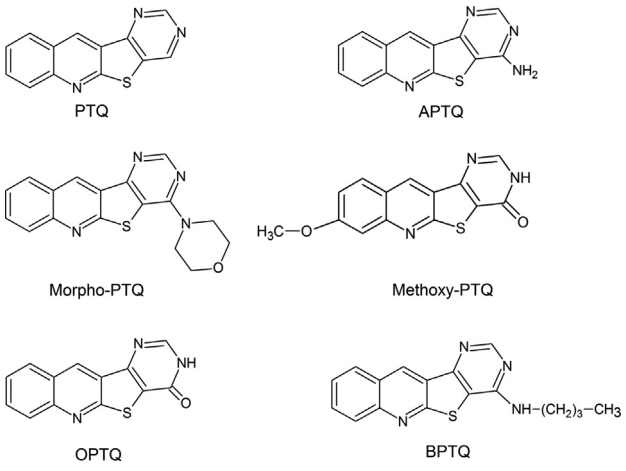

Figure 1 Structures of test compounds used for the study.

2. Materials and methods

2.1. Ligand and receptor preparation

To perform docking studies, ten different kinases receptors (Table 1) were retrieved from the Protein Data Bank (http://www.rcsb.org/). Ligands and water molecules were removed using PyMol molecular visualization software from the retrieved receptor. The three dimen sional chemical structure of standard drug, staurosporine was retrieved from the PubChem (https://pubchem.ncbi.nlm.nih.gov/). The two-dimensional (2D) structure of the test molecules (ligands) was drawn using the software ACD/Chemsketch. This was further followed by hydrogen addition and conversion to 3D structure. All the obtained sdf and mol format files were converted into pdb format files using the Open Babel software.

2.2. Virtual screening by molecular docking

Docking was performed using Hex 6.3 software[19] between the kinases (receptor) and test or standard drugs. To identify the interaction between the receptor and drug, the best solution binding mode is selected out of 2000 possible solutions. Following are the parameters which are used in the controls to perform docking: correlation type: shape + electrostatics; FFT mode: 3D; post processing: MM minimization; grid dimension: 0.4; solutions: 2000; receptor range: 180; step size: 7.5; ligand range: 180; step size: 7.5; twist range: 360; step size: 5.5; distance range: 40; scan step: 0.8; steric scan: 18; final search: 25. After completion of docking calculations, respective energy values were noted and complex structures of both receptor and drug were saved, and visualized in the PyMol molecular visualization software for interactions.

2.3. Reagents

All chemicals unless otherwise mentioned were purchased from Sigma–Aldrich (USA). Fetal bovine serum was obtained from Gibco (USA). Penicillin, streptomycin, annexin V–fluorescein isothiocyanate (FITC) apoptosis detection kit, and propidium iodide were purchased from Invitrogen (USA).

2.4. In vitro primary kinase profiling and IC_{50} determinations

In vitro kinase assays were carried out by performing a radioactive filter binding assay using [γ-^{33}P] ATP in a 96-well format[20,21]. The inhibition potential of BPTQ was tested on ten different PKs, such as aurora A, aurora B, checkpoint kinase 1 (CHK1), checkpoint kinase 2

Table 1 Docking energy values of PTQ derivatives on different kinase receptors.

Target	PDB ID	PTQ	APTQ	BPTQ[a]	Methoxy-PTQ	Morpho-PTQ	OPTQ	Staurosporine
Aurora-A	1MQ4	–234.18	–234.57	–311.85	–278.58	–301.39	–230.63	–344.65
Aurora-B	2VGP	–90.29	–88.01	–111.91	–72.73	–76.1	–90.81	–213.86
CHK1	3TKI	–241.94	–241.58	–322.64	–285.71	–280.33	–241.91	–351.44
CHK2	4A9S	–236.09	–228.62	–333.38	–264.35	–287	–227.72	–348.4
ERK1	2ZOQ	–240.13	–248.06	–301.61	–270.23	–262.87	–240.33	–363.33
MNK1	2HW6	–227.56	–226.36	–312.18	–247.47	–260.75	–224.87	–314.23
MNK2	2HW7	–255.06	–268.15	–307.8	–266.67	–299.35	–262.6	–385.8
PIM1	3BGQ	–250.07	–249.61	–329.32	–286.18	–267.46	–246.67	–302.73
PKBa	1O6K	–245.66	–253.67	–307.02	–263.54	–279.45	–250.5	–346.74
VEGFR1	3HNG	–251.19	–263.11	–307.05	–278.32	–276.15	–263.25	–359.13

[a]Test molecule with lowest docking energy values.

(CHK2), extracellular signal–regulated protein kinase 1 (ERK1), MAP kinase interacting kinase 1 (MNK1), MAP kinase interacting kinase 2α (MNK2α), proto-oncogene serine/threonine-protein kinase (PIM1), protein kinase Bα (PKBα) and vascular endothelial growth factor receptor 1 (VEGFR1). Each kinase activity assay was performed in duplicate with a BPTQ concentration of 1 μmol/L. The assays were initiated by the addition of MgATP, reactions were incubated for 30 min, and stopped by the addition of 5 μL of 0.5 mol/L orthophosphoric acid. Counts are read on a Topcount NXT (PerkinElmer, USA). Percentage of remaining kinase activity was calculated for each PKs. For IC_{50} determination, assay was carried out at ten different concentrations of BPTQ ranging from 0.003 to 100 μmol/L. A panel of known kinase inhibitors was used to compare the efficiency of BPTQ (Table 2).

2.5. *Cell culture and trypan blue assay*

Human promyelocytic leukemia (HL-60) cells were obtained from National Centre for Cell Science (Pune, India) and routinely maintained and grown in RPMI-1640 supplemented with 10% heat inactivated FBS, L-glutamate (2 mmol/L), penicillin (100 IU/mL) and streptomycin (100 μg/mL) at 37 °C containing 5% CO_2 (Eppendorf, Germany). BPTQ stock (50 mmol/L) solution was prepared in dimethyl sulfoxide (DMSO) and diluted with RPMI-1640 to give final concentrations. In all experiments, cells treated with RPMI-1640-diluted DMSO were treated as a control.

The anticancer activity of BPTQ was analyzed using trypan blue exclusion assay as described earlier[22]. Briefly, 5×10^4 exponentially growing HL-60 cells were grown in 24-well plates for 24 h at 37 °C. Cells were treated with increasing concentrations (10, 50, 100 and 250 μmol/L) of BPTQ and collected at an interval of 24 h, and resuspended in 0.4% trypan blue. The number of viable cells was counted by using a hemocytometer.

2.6. *Drug accumulation assay*

Cellular uptake of the drug was determined by measuring the fluorescence emission of BPTQ in cells upon treatment. After incubation in drug-containing medium for 2 h, HL-60 cells were centrifuged and washed with pre-chilled phosphate buffered saline (PBS) before being resuspended in 2 mL of 0.1 mol/L HCl in PBS. Fluorescence was determined with excitation of 288 nm and emission of 446 nm in a fluorescence spectrophotometer (Agilent, USA). Cells without treatment were used as control[23].

Table 2 IC_{50} values of BPTQ and standard drugs against VEGFR1 and CHK2.

Ligand molecule	IC_{50} (μmol/L)[a]	
	VEGFR1	CHK2
BPTQ	0.540 ± 0.16	1.70 ± 0.25
Indirubin	0.042 ± 0.012	0.081 ± 0.019
SP600125	0.335 ± 0.074	0.304 ± 0.094
Staurosporine	0.0058 ± 0.0009	0.013 ± 0.003
K252a	0.013 ± 0.002	0.023 ± 0.005
Myricetin	0.779 ± 0.173	1.986 ± 0.276
Go6975	0.014 ± 0.002	0.131 ± 0.017
Ro318220	0.120 ± 0.014	1.069 ± 0.210

[a]Values are mean ± SD (n = 3).

2.7. *LDH release assay*

Lactate dehydrogenase (LDH) release from a cell is an indicator of loss of membrane integrity. LDH assay was performed by using standard protocols[24]. The release of LDH from cells to medium was assessed for 24, 48 and 72 h following BPTQ treatment (10, 50 and 100 μmol/L) on HL-60 cells.

2.8. *Cell cycle analysis*

Effect of BPTQ on cell cycle distribution was analyzed by flow cytometry after propidium iodide staining[3]. Cells (1×10^6) were grown in 100-mm culture dishes and were treated with 10, 50 and 100 μmol/L of BPTQ for 48 h. The cells were harvested, washed, and resuspended in PBS followed by fixation with 75% ice-cold ethanol. Then, the cells were stored overnight at −20 °C before being washed and resuspended in 500 μL of PBS containing 250 μg/mL of RNase A, and incubated for 3–4 h at 37 °C. Finally, the cells were stained with 50 μg/mL of propidium iodide. Acquisition and analysis of flow cytometry data were carried out using Cell Quest Pro software (FACSCalibur, Becton Dickinson).

2.9. *Annexin V-FITC labeling and confocal imaging*

The annexin V labeling assay was performed by using annexin V-FITC apoptosis detection kit (Invitrogen, USA) as described earlier[25,26]. Briefly, cells were incubated in 5 and 10 μmol/L BPTQ for

48 h. After treatment, cells were washed twice with ice cold PBS and resuspended in 100 µL annexin-binding buffer (10 mmol/L HEPES, 140 mmol/L NaCl, 2.5 mmol/L $CaCl_2$, pH 7.4), and were incubated with 5 µL of FITC-conjugated annexin V and 1 µL of the 100 µg/mL propidium iodide working solution. Cells were then spread over a slide and observed under an inverted confocal laser scanning microscope (Ziess LSM 510 META, Germany).

2.10. *Mitochondrial membrane potential measurement*

Effect of BPTQ on the mitochondrial membrane potential ($\Delta\Psi_m$) of leukemia cells was determined by performing 5,5′,6,6′-tetrachloro-1,1′,3,3′-tetraethyl benzimidazolcarbo-cyanamide iodide (JC-1) staining[27]. HL-60 cells (1×10^5) were cultured and treated with 10 µmol/L BPTQ. After incubation at different time points, cells were washed and labeled for 45 min with 10 µmol/L JC-1 at 37 °C before being washed three times and resuspended in PBS. Changes in the fluorescence were monitored at 530 and 590 nm. The ratio of the red fluorescence of JC-1 aggregates (590 nm) to green fluorescence of diluted JC-1 (530 nm) was considered as the relative $\Delta\Psi_m$ value.

2.11. *Caspase-3 activity*

The caspase-3 activity assay was performed using caspase-3 colorimetric assay kit (Sigma, USA) following the manufacturer's suggested protocol. Briefly, cell were treated for 48 h with 10 µmol/L BPTQ and washed with PBS. The pellet was suspended in 1 × lysis buffer and incubated on ice for 15 min, followed by centrifugation at 20,000 × *g* for 15 min at 4 °C. The supernatant was collected. Samples were mixed with assay buffer with or without caspase-3 inhibitor (Ac-DEVD-CHO). Finally, caspase-3 substrate, acetyl-Asp-Glu-Val-Asp-*p*-nitroanilide (Ac-DEVD-*p*NA) was added to all the samples and incubated at 37 °C for 90 min. Absorbance was recorded at 405 nm. The caspase activity was represented as the concentration of pNA formed per min per mL of cell lysate.

3. Results

3.1. *Computational studies*

In search of novel protein kinase inhibitors, we performed the molecular docking of PTQ molecules possessing different functional groups with ten different kinase receptors such as Aurora A, Aurora B, CHK1, CHK2, ERK1, MNK1, MNK2α, PIM1, PKBα and VEGFR1. Virtual screening of six PTQ derivatives confirmed that all the test molecules differentially bind to the receptors. To evaluate the potency of test molecules, we compare their docking energy values with the standard molecule (Table 1). Among the test molecules, BPTQ emerged as top scoring by showing lowest docking energy value with all the receptors. BPTQ displayed both induced fit (Fig. 2A and B) and hydrogen bonding interaction (Fig. 2C and D) depending on the receptors. BPTQ showed hydrogen bonding interaction with ARG 1120 and GLU 1123 residues of VEGFR1. Staurosporine was used as a standard molecule, which showed more effective binding interactions with the receptors (Fig. 2E and F) even than that of BPTQ (Table 1). These data may corroborate that BPTQ is an effective inhibitor of kinases, but comparatively less effective than staurosporine. As BPTQ is an effective inhibitor compared to the other test molecules, we selected it to perform the *in vitro* kinase inhibition screening and anticancer studies.

3.2. *Identification of potential target of BPTQ in vitro*

Ten different PKs were selected for identifying the potential target of BPTQ. The *in vitro* kinase inhibitory activity of BPTQ was evaluated at a concentration of 1 µmol/L by performing the radiometric kinase assay. The percent kinase inhibition after BPTQ treatment was calculated. Encouragingly, BPTQ inhibited seven kinases out of ten targets selected for this study (Fig. 3A). Strong inhibition of VEGFR1 and CHK2 with the percent inhibition of

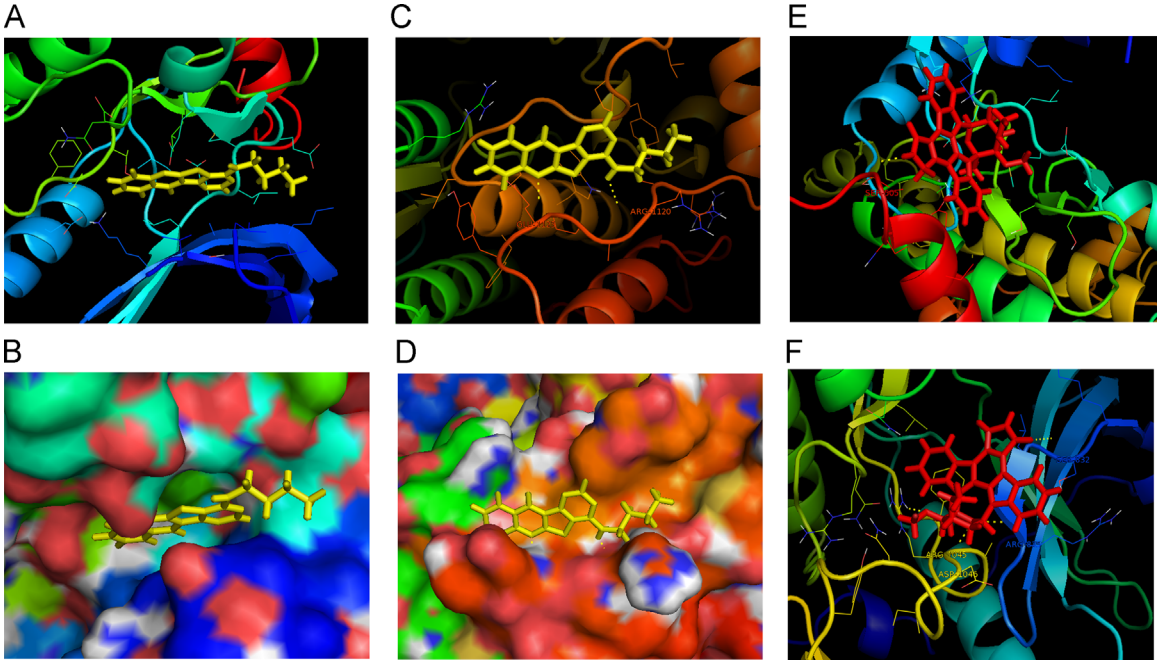

Figure 2 Molecular docking of BPTQ and staurosporine with CHK2 and VEGFR1 receptor. Molecular interaction of BPTQ with CHK2 (A and B) and VEGFR1 (C and D); molecular interaction of staurosporine with CHK2 (E) and VEGFR1 (F).

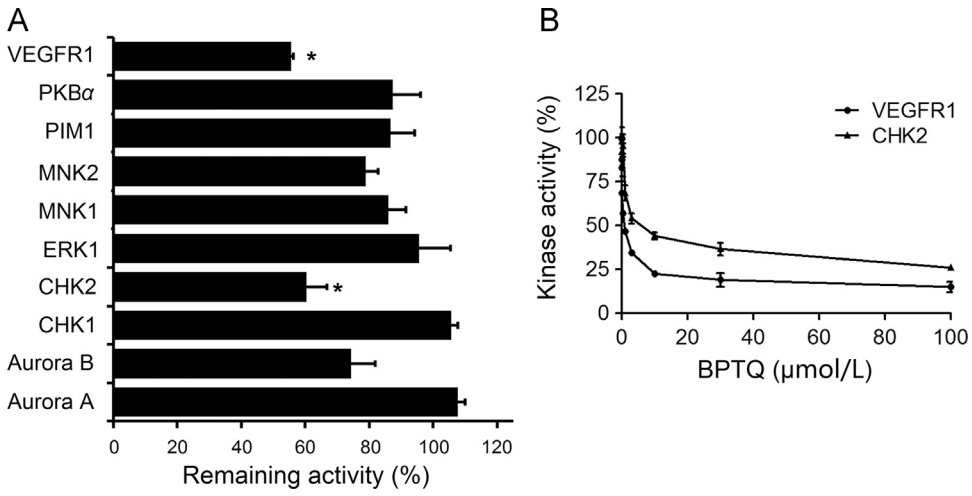

Figure 3 *In vitro* primary kinase profiling and dose–response curve of BPTQ on CHK2 and VEGFR1. (A) Bar diagram showing the kinase activity (%) of a panel of protein kinases tested with 1 μmol/L BPTQ using an *in vitro* assay; (B) dose response curve of BPTQ on CHK2 and VEGFR1.

44% and 40%, respectively, was observed along with moderate inhibition of Aurora B (74%) and MNK2 (79%). Limited or no inhibition was observed for other kinases. Therefore, it is confirmed that, BPTQ is more effective against VEGFR1 and CHK2 compared to other PKs used.

The dose response curve for VEGFR1 and CHK2 at ten different concentrations of BPTQ was subsequently determined (Fig. 3B). IC_{50} values of 0.54 ± 0.16 μmol/L and 1.70 ± 0.25 μmol/L on VEGFR1 and CHK2, respectively, were determined for BPTQ from two independent tests. This is in the range of a panel of known kinase inhibitors (Table 2). Staurosporine showed more strong inhibition against VEGFR1 ($IC_{50} = 5.8$ nmol/L) and CHK2 ($IC_{50} = 13.32$ nmol/L) than that of BPTQ. This is in agreement with the docking study where staurosporine showed a strong interaction with these kinases than BPTQ.

3.3. *Cytotoxicity studies*

The anti-proliferative ability of BPTQ on HL-60 cell line was measured by trypan blue assay. We observed dose-dependent cytotoxicity against HL-60 cells for BPTQ (Fig. 4A) with an IC_{50} of 12 μmol/L at 48 h. This confirms that BPTQ possess anti-proliferative activity on HL-60 cells. Accumulation of BPTQ in HL-60 cells was analyzed by measuring the fluorescence emission of BPTQ at 446 nm (excitation at 288 nm) in treated and untreated cells. After 2 h of incubation with BPTQ, treated cells showed a dose dependent increase in the intracellular drug uptake compared to drug free control (Fig. 4B).

Further, cytotoxicity was also confirmed by estimating the release of lactate dehydrogenase enzyme from cells. Treatment BPTQ at 10 μmol/L did not induce LDH release in HL-60 cells. At concentrations of 50 and 100 μmol/L, BPTQ increased the release of LDH from HL-60 cells (Fig. 4C), suggesting cytolysis only at higher concentrations of BPTQ treatment. As the cytolysis is an indicator of necrotic cell death, minimal cytolysis at 10 μmol/L treatment might suggest an apoptotic mode of cell death for BPTQ.

3.4. *BPTQ induces apoptosis in HL-60 cells*

Flow cytometry was used to investigate whether the inhibition of HL-60 proliferation by BPTQ was mediated by regulating cell cycle progression. HL-60 cells showed the typical cell cycle distribution with ~50% cells in G0/G1 phase, 28% cells in S-phase, and ~16% cells in G2/M phase (Fig. 5A). Dose response effect of BPTQ at 48 h of treatment was analyzed. Treatment did not induce any cell cycle arrest, but resulted in strong apoptotic response as the number of cells in sub-G0/G1 populations (hypodiploid apoptotic cells) increased to 47% with concomitant decrease in G0/G1, S and G2/M populations

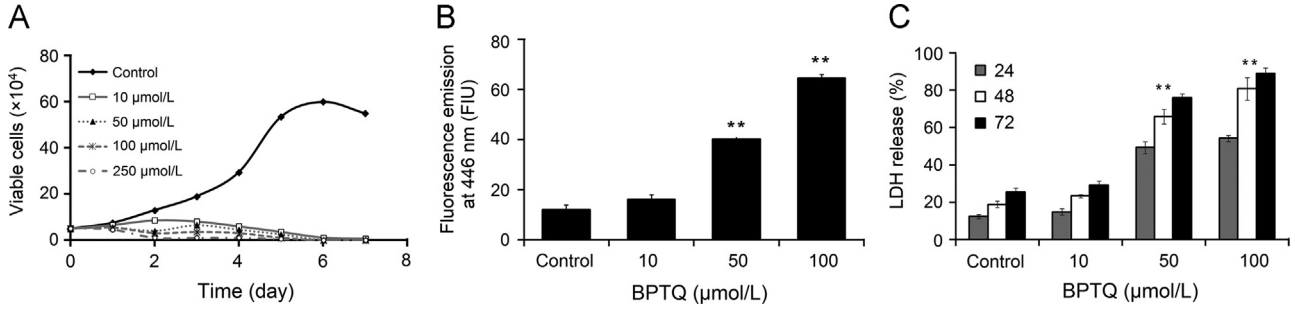

Figure 4 Effect of BPTQ on the proliferation of HL-60 cells. (A) Line diagram showing cytotoxicity of BPTQ on HL-60 cell line. HL-60 cells were incubated with different concentrations of BPTQ for different time points and number of viable cells was determined by trypan blue assay. (B) Accumulation of BPTQ to HL-60 cells. FIU, fluorescence intensity unit. (C) Cytotoxicity measured as LDH release upon BPTQ treatment. In all panels, error bars indicates ± SD ($n = 3$). $^{**}P < 0.01$, a significant difference from the controls.

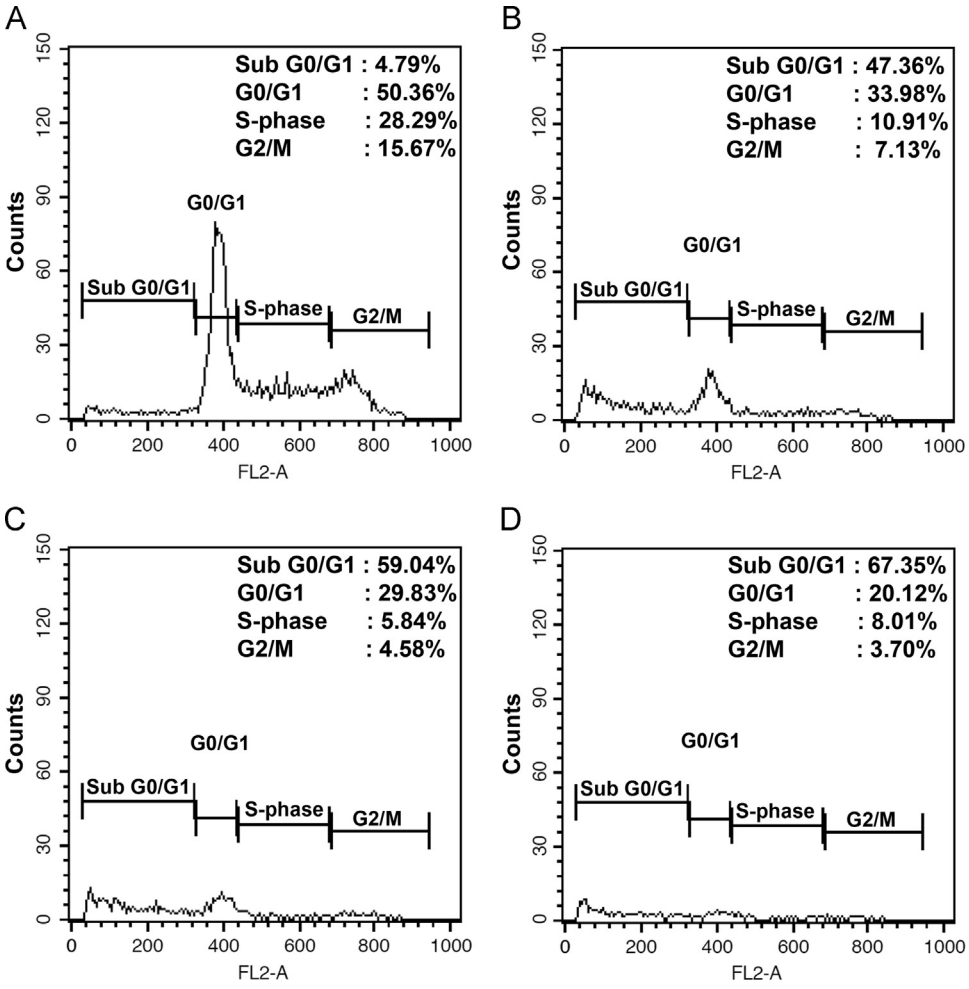

Figure 5 Effect of BPTQ on the cell cycle distribution of HL-60 cells analyzed using flow cytometry. The experiment was repeated three times and representative histograms are shown. (A) Control; (B) BPTQ 10 μmol/L; (C) BPTQ 50 μmol/L; (D) BPTQ 100 μmol/L.

at 10 μmol/L (Fig. 5B). Further, treatment with higher concentration of BPTQ (50 and 100 μmol/L) killed most of the cells in a dose dependent manner (Fig. 5C and D). About 68% of apoptotic (sub-G0/G1) cells were observed after treating with 100 μmol/L.

To confirm the induction of apoptosis by BPTQ, we performed annexin V-FITC and propidium iodide double staining, and analyzed by confocal microscopy. Untreated cells did not show any of the fluorescence. But many of the cells treated with BPTQ were stained with either annexin V-FITC alone (early apoptosis) or by both annexin V-FITC and propidium iodide dye (late apoptosis), confirming the induction of apoptosis by BPTQ (Fig. 6A).

As mitochondria have been shown to play a major role in apoptosis, depolarization of mitochondrial membrane potential ($\Delta\Psi_m$) of leukemia cells upon BPTQ treatment was evaluated using the JC-1 dye. A striking fall in the membrane potential was observed following BPTQ treatment ($P<0.01$, Fig. 6B). The downfall in $\Delta\Psi_m$ started as early at 6 h and continued as time lapsed. NAC pre-incubation did not reverse the fall in $\Delta\Psi_m$, ruling out the role of ROS in the collapse of $\Delta\Psi_m$.

Disruption of mitochondrial membrane potential often leads to the activation of caspases. Activation of an effector caspase, caspase-3 upon BPTQ treatment was investigated in HL-60 cells by using a colorimetric substrate. Results confirmed that, BPTQ treatment has significantly increased the intracellular caspase-3 activity compared to control ($P<0.01$). The increase in the caspase-3 activity was about 2-fold to that of control. Treatment with caspase-3 specific inhibitor (Ac-DEVD-CHO) reversed the activation, confirming that the observed activity was by caspase-3 and not by other non-caspase proteases (Fig. 6C). Therefore, it is confirmed that the apoptosis induced by BPTQ in HL-60 cells is caspase dependent.

4. Discussion

About 518 PKs have been identified in the human genome[28,29], which includes 90 tyrosine kinases. These tyrosine kinases are again classified into receptor tyrosine kinases (RTKs) and non-receptor tyrosine kinases (NRTKs). About 58 RTKs and 32 NRTKs have been identified so far[10]. The association of many of the RTKs and NRTKs in cancer is well known. Since these human protein tyrosine kinases play a central role in carcinogenesis, they have emerged as the promising targets to develop novel anticancer drugs. Therefore, several protein kinase inhibitors have been developed with impressive preclinical anticancer effects[30].

In silico molecular docking analysis has been widely used to screen the molecules with biological activity based on the interaction of test molecules with various receptors. These docking analyses also help in screening the best molecule in the lot and to carry out further *in vitro* studies. Results showed that, all the six

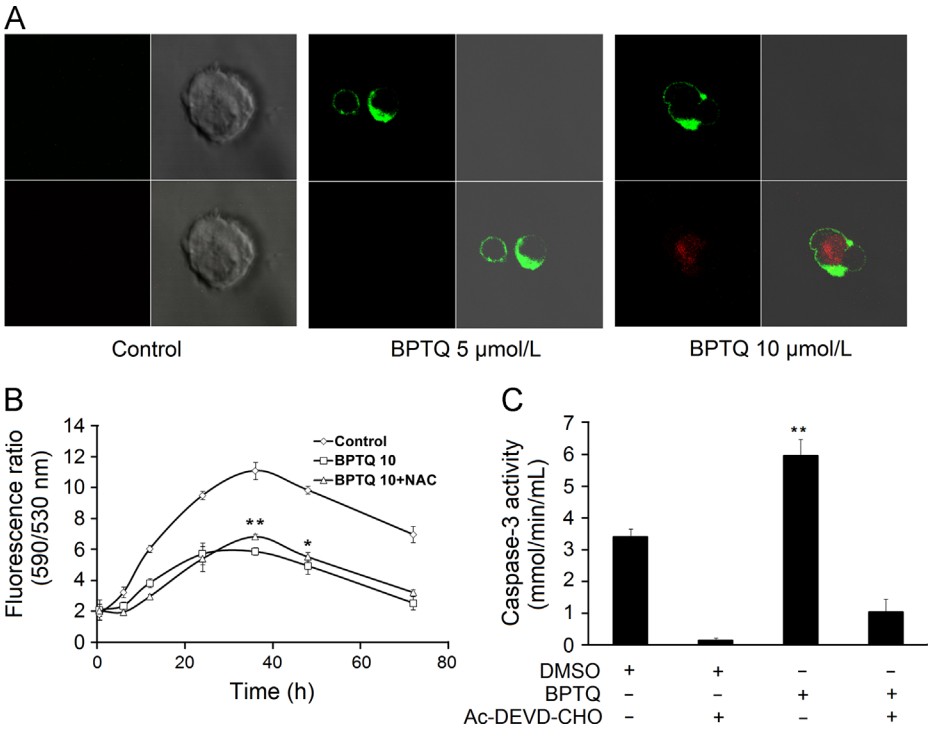

Figure 6 Evaluation of cell death mode induced by BPTQ in HL-60 cells. (A) Cells were visualized by confocal microscopy after staining with fluorescein isothiocyanate-conjugated annexin V and propidium iodide. Left panel, untreated control cells; Middle panel, cells treated with 5 μmol/L BPTQ; Right panel, cells treated with 10 μmol/L BPTQ. (B) Effect of BPTQ on mitochondrial membrane potential. (C) Effect of BPTQ on caspase-3 expression. Values were expressed as the concentration of pNA formed per min per mL of cell lysate. Error bars indicate ± SD ($n=3$). *$P<0.05$, **$P<0.01$; significance is compared with the control group.

test molecules possess differential binding efficiency as depicted by their docking energy values. Though, all the test molecules belonged to the same class of PTQs, they displayed a varying degree of interactions with each receptor. This may probably due to the different functional group present in each molecule.

We further selected the molecule with lowest docking energy, BPTQ for further *in vitro* kinase inhibition studies. *In vitro* inhibition studies confirmed that BPTQ inhibits CHK2 and VEGFR1 effectively than other PKs studied. Though the IC_{50} value of BPTQ is less than staurosporine, it is in the range of panel of known kinase inhibitors. The inhibition of CHK2 was earlier reported to sensitize malignant cells to apoptosis[31]. Also, the VEGFR1 was known to be a potential target in leukemia and other cancer forms, and the inhibition of VEGFR1 reported to induce apoptosis in leukemia cells[32–34]. This is because the VEGF acts as a growth factor in leukemic cells like MOLT-4, and cells express VEGFR1 receptors on their cell surfaces[33]. Thus, these results reveal one of the possible mechanisms of anticancer and apoptotic activity of BPTQ on MOLT-4 cells, which was reported earlier[16]. It is hypothesized that kinase inhibitory ability of BPTQ might also contribute along with DNA intercalation to its antiproliferative activity. This is on the lines of the DNA intercalator mitoxantrone, which also possess kinase inhibitory activity[17].

Further, we studied the anti-proliferative effects of BPTQ on HL-60 cells. We observed dose-dependent cytotoxicity against HL-60 with no cell cycle arrest. This was in contrast to the result against MOLT-4 cells where the cell cycle arrest was observed[16], suggesting differential activity possessed by BPTQ on different cell lines. Further, mode of cell death induced by BPTQ was through the mitochondrial mediated apoptotic pathway. This was confirmed through annexin V/PI double staining, mitochondrial membrane potential and caspase activity assays. Also, increase of cell proportion in the sub G0/G1 phase upon BPTQ treatment provides further evidence to the apoptotic mode of cell death. This is in agreement with that of commonly used chemotherapeutic drugs which induce apoptosis in malignant cells[35,36]. The depolarization of mitochondria membrane in human leukemia cells upon BPTQ treatment was also observed. This confirms the role of mitochondria in apoptosis, since the opening of the mitochondrial permeability transition pore is associated with mitochondria-mediated apoptotic cell death processes[37]. Taken together, these data corroborates that the BPTQ also possess ability to inhibit VEGFR1 and CHK2, and induces apoptosis in HL-60 cells.

5. Conclusions

In this study, we report that BPTQ inhibits VEGFR1 and CHK2 as depicted by molecular docking and *in vitro* studies. BPTQ also possess antiproliferative activity on HL-60 cells. The inhibition of cancer cell proliferation by BPTQ is through mitochondrial mediated apoptotic cell death process. This study will shed light on the novel targets of DNA intercalative molecules, which may be useful in the development of new therapeutic molecules in the future.

Acknowledgments

This work was supported by grant BT/PR10513/BRB/10/618/2008 to GMA from Department of Biotechnology (DBT), Ministry of

Science and Technology, Government of India (New Delhi). FACS and confocal facilities of C-CAMP, NCBS are also acknowledged. HGR was supported by DBT (India).

References

1. Sadikovic B, Al-Romaih K, Squire JA, Zielenska M. Cause and consequences of genetic and epigenetic alterations in human cancer. *Curr Genomics* 2008;**9**:394–408.
2. Robison K. Application of second-generation sequencing to cancer genomics. *Brief Bioinform* 2010;**11**:524–34.
3. Shahabuddin MS, Nambiar M, Choudhary B, Advirao GM, Raghavan SC. A novel DNA intercalator, butylamino-pyrimido[4′,5′:4,5]selenolo (2,3-*b*)quinoline, induces cell cycle arrest and apoptosis in leukemic cells. *Invest New Drugs* 2010;**28**:35–48.
4. Pearson MA, Fabbro D. Targeting protein kinases in cancer therapy: a success?. *Expert Rev Anticancer Ther* 2004;**4**:1113–24.
5. Hanahan D, Weinberg RA. The hallmarks of cancer. *Cell* 2000;**100**:57–70.
6. Hanahan D, Weinberg RA. Hallmarks of cancer: the next generation. *Cell* 2011;**144**:646–74.
7. Arora A, Scholar EM. Role of tyrosine kinase inhibitors in cancer therapy. *J Pharmacol Exp Ther* 2005;**315**:971–9.
8. Faivre S, Djelloul S, Raymond E. New paradigms in anticancer therapy: targeting multiple signaling pathways with kinase inhibitors. *Semin Oncol* 2006;**33**:407–20.
9. Chang F, Steelman LS, Lee JT, Shelton JG, Navolanic PM, Blalock WL, et al. Signal transduction mediated by the Ras/Raf/MEK/ERK pathway from cytokine receptors to transcription factors: potential targeting for therapeutic intervention. *Leukemia* 2003;**17**:1263–93.
10. Madhusudan S, Ganesan TS. Tyrosine kinase inhibitors in cancer therapy. *Clin Biochem* 2004;**37**:618–35.
11. Nichols GL. Tyrosine kinase inhibitors as cancer therapy. *Cancer Invest* 2003;**21**:758–71.
12. Gopal M, Shenoy S, Doddamani LS. Antitumor activity of 4-amino and 8-methyl-4-(3-diethylamino propylamino)pyrimido[4′,5′:4,5]thieno(2,3-*b*)quinolines. *J Photochem Photobiol B Biol* 2003;**72**:69–78.
13. Shahabuddin MS, Gopal M, Raghavan SC. Intercalating, cytotoxic, antitumour activity of 8-chloro and 4-morpholinopyrimido[4′,5′:4,5] thieno(2,3-*b*)quinolines. *J Photochem Photobiol B* 2009;**94**:13–9.
14. Gopal M, Shahabuddin MS, Inamdar SR. Interaction between an 8-methoxypyrimido[4′,5′:4,5]thieno(2,3-*b*)quinoline-4(3*H*)one antitumour drug and deoxyribonucleic acid. *J Chem Sci* 2002;**114**:687–96.
15. Shahabuddin MS, Gopal M, Sathees RC. Intercalating and antitumour activity of 4-oxopyrimido[4′,5′:4,5]thieno(2,3-*b*)quinoline-4(3*H*)-one. *J Cancer Mol* 2007;**3**:139–46.
16. RohitKumar HG, Asha KR, Raghavan SC, Advi Rao GM. DNA intercalative 4-butylaminopyrimido[4′,5′:4,5]thieno(2,3-*b*)quinoline induces cell cycle arrest and apoptosis in leukemia cells. *Cancer Chemother Pharmacol* 2015;**75**:1121–33.
17. Wan X, Zhang W, Li L, Xie Y, Li W, Huang N. A new target for an old drug: identifying mitoxantrone as a nanomolar inhibitor of PIM1 kinase *via* kinome-wide selectivity modeling. *J Med Chem* 2013;**56**:2619–29.
18. Stasevych M, Zvarych V, Lunin V, Halenova T, Savchuk O, Dudchak O, et al. Novel anthraquinone-based derivatives as potent inhibitors for receptor tyrosine kinases. *Indian J Pharm Sci* 2015;**77**:634–7.
19. Ritchie DW, Kemp GJ. Protein docking using spherical polar Fourier correlations. *Proteins* 2000;**39**:178–94.
20. Hastie CJ, McLauchlan HJ, Cohen P. Assay of protein kinases using radiolabeled ATP: a protocol. *Nat Protoc* 2006;**1**:968–71.
21. Bain J, Plater L, Elliott M, Shpiro N, Hastie CJ, Mclauchlan H, et al. The selectivity of protein kinase inhibitors: a further update. *Biochem J* 2007;**408**:297–315.
22. Hegde M, Karki SS, Thomas E, Kumar S, Panjamurthy K, Ranganatha SR, et al. Novel levamisole derivative induces extrinsic pathway of apoptosis in cancer cells and inhibits tumor progression in mice. *PLoS One* 2012;**7**:e43632.
23. Egorin MJ, Clawson RE, Ross LA, Schlossberger NM, Bachur NR. Cellular accumulation and disposition of aclacinomycin A. *Cancer Res* 1979;**39**:4396–400.
24. Kavitha CV, Nambiar M, Ananda Kumar CS, Choudhary B, Muniyappa K, Rangappa KS, et al. Novel derivatives of spirohydantoin induce growth inhibition followed by apoptosis in leukemia cells. *Biochem Pharmacol* 2009;**77**:348–63.
25. Vermes I, Haanen C, Steffens-Nakken H, Reutellingsperger C. A novel assay for apoptosis flow cytometric detection of phosphatidylserine expression on early apoptotic cells using fluorescein labelled annexin V. *J Immunol Methods* 1995;**184**:39–51.
26. Mukhopadhyay P, Rajesh M, Haskó GP, Hawkins BJ, Madesh M, Pacher P. Simultaneous detection of apoptosis and mitochondrial superoxide production in live cells by flow cytometry and confocal microscopy. *Nat Protoc* 2007;**2**:2295–301.
27. Mehta A, Shaha C. Mechanism of metalloid-induced death in *Leishmania* spp.: role of iron, reactive oxygen species, Ca^{2+}, and glutathione. *Free Radic Biol Med* 2006;**40**:1857–68.
28. Manning G, Whyte DB, Martinez R, Hunter T, Sudarsanam S. The protein kinase complement of the human genome. *Science* 2002;**298**:1912–34.
29. Krupa A, Srinivasan N. The repertoire of protein kinases encoded in the draft version of the human genome: atypical variations and uncommon domain combinations. *Genome Biol* 2002;**3** research0066.1.
30. Vanneman M, Dranoff G. Combining immunotherapy and targeted therapies in cancer treatment. *Nat Rev Cancer* 2012;**12**:237–51.
31. Castedo M, Perfettini JL, Roumier T, Yakushijin K, Horne D, Medema R, et al. The cell cycle checkpoint kinase Chk2 is a negative regulator of mitotic catastrophe. *Oncogene* 2004;**23**:4353–61.
32. Wegiel B, Ekberg J, Talasila KM, Jalili S, Persson JL. The role of VEGF and a functional link between VEGF and $p27^{Kip1}$ in acute myeloid leukemia. *Leukemia* 2009;**23**:251–61.
33. Broggini M, Marchini SV, Galliera E, Borsotti P, Taraboletti G, Erba E, et al. Aplidine, a new anticancer agent of marine origin, inhibits vascular endothelial growth factor (VEGF) secretion and blocks VEGF-VEGFR-1 flt-1 autocrine loop in human leukemia cells MOLT-4. *Leukemia* 2003;**17**:52–9.
34. Biscardi M, Caporale R, Balestri F, Gavazzi S, Jimeno J, Grossi A. VEGF inhibition and cytotoxic effect of aplidin in leukemia cell lines and cells from acute myeloid leukemia. *Ann Oncol* 2005;**16**:1667–74.
35. Cheah YH, Nordin FJ, Sarip R, Tee TT, Azimahtol HL, Sirat HM, et al. Combined xanthorrhizol-curcumin exhibits synergistic growth inhibitory activity *via* apoptosis induction in human breast cancer cells MDA-MB-231. *Cancer Cell Int* 2009;**9**:1.
36. Fleischer A, Ghadiri A, Dessauge F, Duhamel M, Rebollo MP, Alvarez-Franco F, et al. Modulating apoptosis as a target for effective therapy. *Mol Immunol* 2006;**43**:1065–79.
37. Kroemer G, Galluzzi L, Brenner C. Mitochondrial membrane permeabilization in cell death. *Physiol Rev* 2007;**87**:99–163.